PROCEEDINGS OF SPIE

SPIEDigitalLibrary.org/conference-proceedings-of-spie

Improvement of the light-tissue coupling for better outcome of phototherapies

Dilleys Ferreira da Silva, José Dirceu Vollet Filho, Thereza Cury Fortunato, Lilian Tan Moriyama, Clovis Grecco, et al.

Dilleys Ferreira da Silva, José Dirceu Vollet Filho, Thereza Cury Fortunato, Lilian Tan Moriyama, Clovis Grecco, Sebastião Pratavieira, Cristina Kurachi, Vanderlei Salvador Bagnato, "Improvement of the light-tissue coupling for better outcome of phototherapies," Proc. SPIE 10476, Optical Methods for Tumor Treatment and Detection: Mechanisms and Techniques in Photodynamic Therapy XXVII, 1047614 (12 February 2018); doi: 10.1117/12.2288515



Event: SPIE BiOS, 2018, San Francisco, California, United States

Improvement of the light-tissue coupling for better outcome of phototherapies

Dilleys Ferreira da Silva; José Dirceu Vollet Filho; Thereza Cury Fortunato; Lilian Tan Moriyama; Clovis Grecco; Sebastião Pratavieira; Cristina Kurachi; Vanderlei Salvador Bagnato University of São Paulo, São Carlos Institute of Physics, PO Box 369, São Carlos, SP, Brazil

ABSTRACT

Phototherapies have been increasingly used in several applications such as the control of pain and inflammatory processes, photodynamic therapy, and even aesthetics uses. After many decades, the dosimetry for those techniques remains challenging. One of the key issues is the lack of homogeneity obtained for tissue illumination, which may limit adequate treatment. Especially concerning lesions, the surface tissue is usually irregular, and the light does not couple to the tissue efficiently to promote an effective treatment. A series of experiments have been performed using optical phantoms, in which coupling was improved by introducing a gel with a low concentration of scattering agents between the fiber and the phantom as an attempt to improve the homogeneity of light distribution within the phantoms. The effects promoted by roughness on phantom tissue surfaces are considerably attenuated when the coupling gel was introduced, resulting in a more uniform illumination pattern that may be used to promote better phototherapy treatments outcome.

Keywords: light-tissue coupling; optical phantoms; dosimetry; carbopol hydrogel

*lili@ifsc.usp.br; http://cepof.ifsc.usp.br/

I. INTRODUCTION

Biological tissues are considered turbid media, in which light scattering effect is much stronger than absorption. Studies on light propagation and distribution in biological media are essential for the improvement of dosimetry of several applications, be it therapy or diagnosis, and several papers can be found in literature exploring mathematical modeling and empirical measurements in order to better understand how light propagates in biological media. ^{1–6} However, most of them do not discuss and explore surface features of biological tissue. Most part of diagnosis and therapeutic applications of light have the skin as target tissue and, we know that skin features (color, texture, topography, hydration, etc.) greatly vary from site to site and from patient to patient, influencing the results.

For phototherapy, photodynamic therapy (PDT) and photodiagnosis applications, the conventional procedure is based on the direct application of a light beam on the skin, an illumination procedure that works well for several applications, however, it can be a limitation in others. For PDT of planar lesions with smooth surface, for instance, conventional irradiation is appropriate, however, for bulky tumors with irregular surface (irregular topography and irregular pigmentation) different illumination strategies should be implemented.

Most part of the studies on light propagation in biological tissues (or turbid media) does not consider the surface features of it. Surface irregularities may lead to a non-uniform light distribution pattern, with shadow effects that may compromise the establishment of a correct dosimetry. For PDT, these irregularities may result in recurrence, since it is crucial to delivery enough light (higher than the threshold dose) to promote death of the whole lesion. For LLLT the expected effect (pain control, inflammation control, cell proliferation) is obtained only when minimum amounts of light are delivered. For this reason, it is important to seek for the improvement of light delivery techniques that allow to create a more controlled dosimetry. A relatively straightforward way to improve the light delivery is using a coupling agent at the tissue interface. It may promote a better refractive index matching, which will result in less reflection. The use of hidrogel, for example, as coupling agent is common for applications like photo-epilation ultrasound therapy and imaging and others.

Optical Methods for Tumor Treatment and Detection: Mechanisms and Techniques in Photodynamic Therapy XXVII, edited by David H. Kessel, Tayyaba Hasan, Proc. of SPIE Vol. 10476, 1047614 · © 2018 SPIE · CCC code: 1605-7422/18/\$18 · doi: 10.1117/12.2288515

In the present study we purpose the use of a gel to improve the light coupling to the tissue and to improve the uniformity of the illumination spot at the tissue interface. Our proposal differs from schemes of coupling light by the action of osmotic agents²⁰ since here, the chosen coupling medium is an inert Hydrogel that does not interact or change the tissue, and preserves its structures. We performed measurements of the light coupling to optical phantom in different situations, imaging the light distribution within the phantom when hidrogel is used in different conditions as coupling agent. A brief discussion on the consequences of our results to PDT e phototherapies is presented.

II. MATERIALS AND METHODS

A turbid optical phantom was created to simulate biological tissue optical properties. The phantom was prepared using 2g of Agar dissolved in 100 ml water, with 20 μ l Lipofundin \mathbb{R}^{21} and 40 μ l of India Ink 22,23 . The phantom was placed in a glass container and to simulate a lesion, a mold with dimensions 2.5 x 1.5 x 1.5 cm, was inserted in the phantom. After the phantom solidification at room temperature, the mold was removed creating the hollow cavity (Figure 1 B); and in order to create an irregular surface at the bottom of the cavity, grooves were manually created. As a light coupling medium, Carbopol hydrogel was used 24 . The refractive indexes of the carbopol gel alone, the carbopol gel plus Lipofundin, and the Agar phantom were measured to show that the indexes are close enough for the aimed application (1.333 for the phantom, and 1.338 for both gel alone and gel with Lipofundin).

A schematic diagram of the experimental setup is shown in Figure 1. The light source used to illuminate the phantom was a diode laser (Eagle Heron® Quantum Tech, São Carlos, Brazil) centered at 630 nm, coupled into a multimode Gaussian optical fiber, NA= 0,2 (FT030, Thorlabs, USA). The optical fiber was positioned 3cm above the phantom surface so that the whole bottom area of the cavity was illuminated.

To evaluate light propagation within the phantom, with or without gel in the cavity, images were acquired using a USB camera, Avantscope Max (1.3 Mega Pixel; Avantgarde) (Avantgarde) 25 . To avoid saturation, the exposure time was set 2 ms. The collected images were analyzed using the software Matlab 7.8®. Three conditions of light coupling to the phantom were evaluated: air-phantom interface (NG); a transparent gel-phantom interface (G); and scattering gel-phantom interface (SG). The scattering gel was prepared adding a little amount of Lipofundin® to the Carpobol gel resulting in $0.4\mu l$ of Lipofundin® per gram of gel.

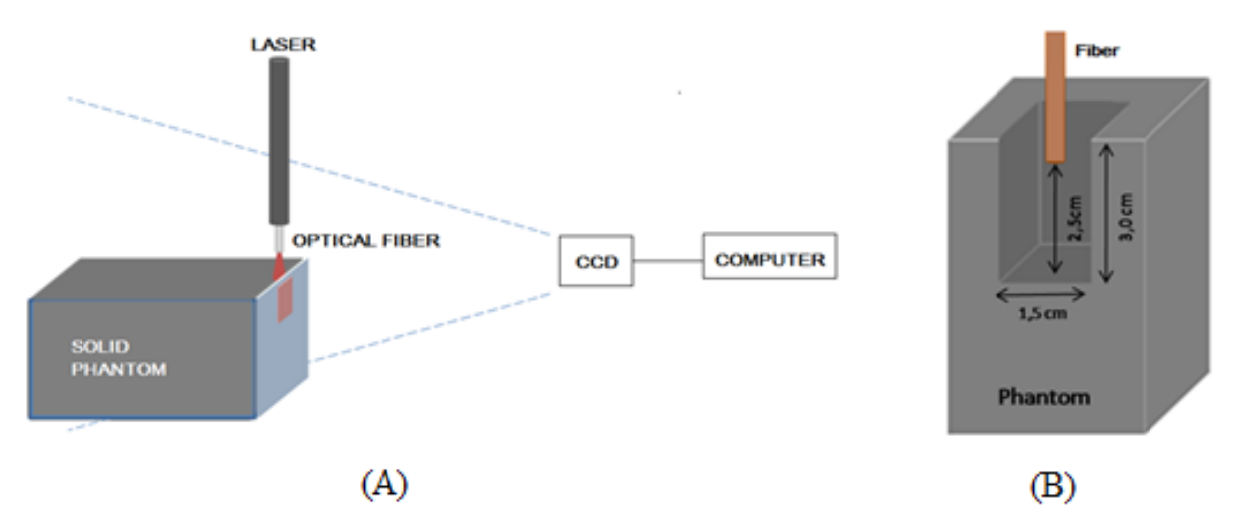


Figure 1: Scheme of experimental setup to evaluate light coupling to the optical phantom. (a) scheme of the experimental setup. (b) detail on the hollow cavity.

III. RESULTS

From the collected images, we extracted the beam profiles and the illumination depth, which are important factors to characterize the efficacy of phototherapies in general. Examples of the beam propagation within the phantom without the coupling gel, within the coupling gel alone, and with the coupling gel plus Lipofundin are shown in Figure 2. The presence of the coupling gel both with and without the scatterer produced a more homogeneous beam distribution as light penetrates the phantom.

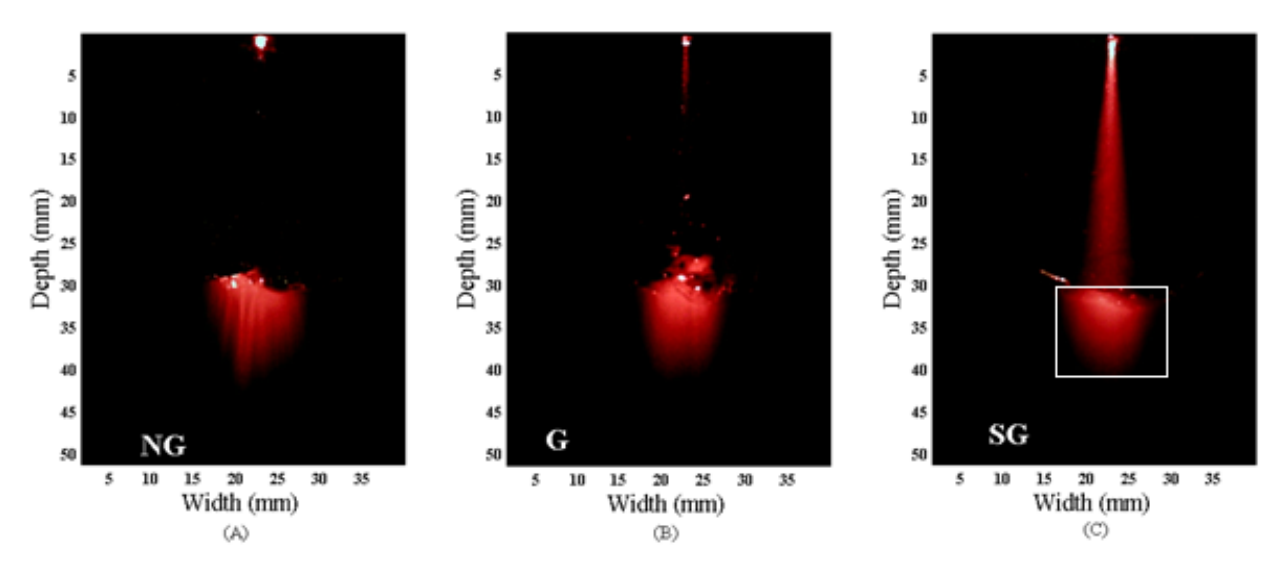


Figure 2: Images of light propagation, with exposure time of 2 ms, in the phantom without gel (NG), with gel only (G), and with gel + scattering agent Lipofundin® (SG). The white square corresponds to the analyzed area beyond the hollow inside the phantom.

To characterize the beam in the phantom, we measured the light profile beyond the interface. The white rectangle in Figure 2(c), corresponds to the area where the light profile was analyzed to characterize the beam profile, after the interface. The presence of the Lipofundin® increases the light scattering together with the index matching²¹. The images for these configurations are shown in Fig 3.

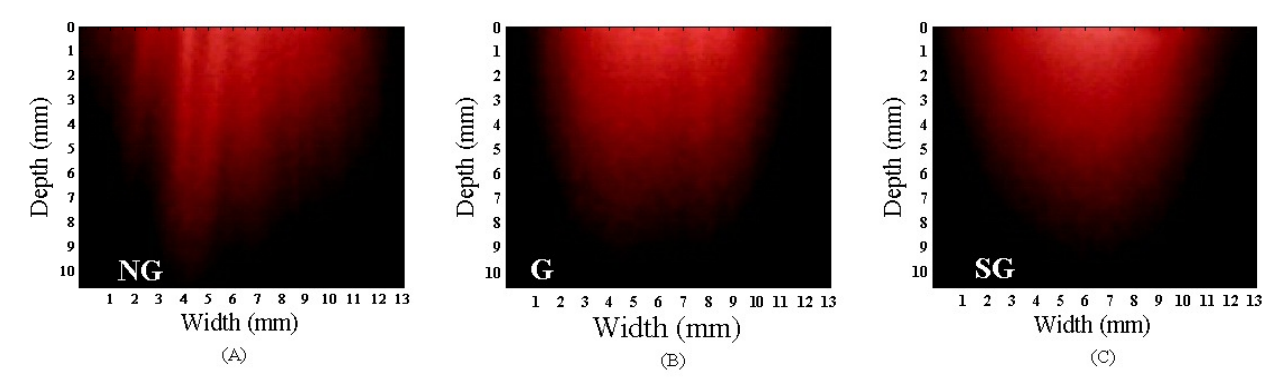


Figure 3: Light profile in the phantom without gel inside the cavity (NG), with gel only (G), and with gel plus 0.4 µl/g of the scattering agent Lipofundin®(SG).

The analysis of the profiles of Figure 3 reveals that the distribution of light in SG exhibits a more uniform and regular spatial profile than the other two configurations. This result is better observed in the "isodose" curves in Figure 4. These isodose curves are a suitable method of mapping the light distribution over the investigated cross-sectioned plane. It is clear from Fig.4A the irregularity of light distribution when no coupling medium was used.

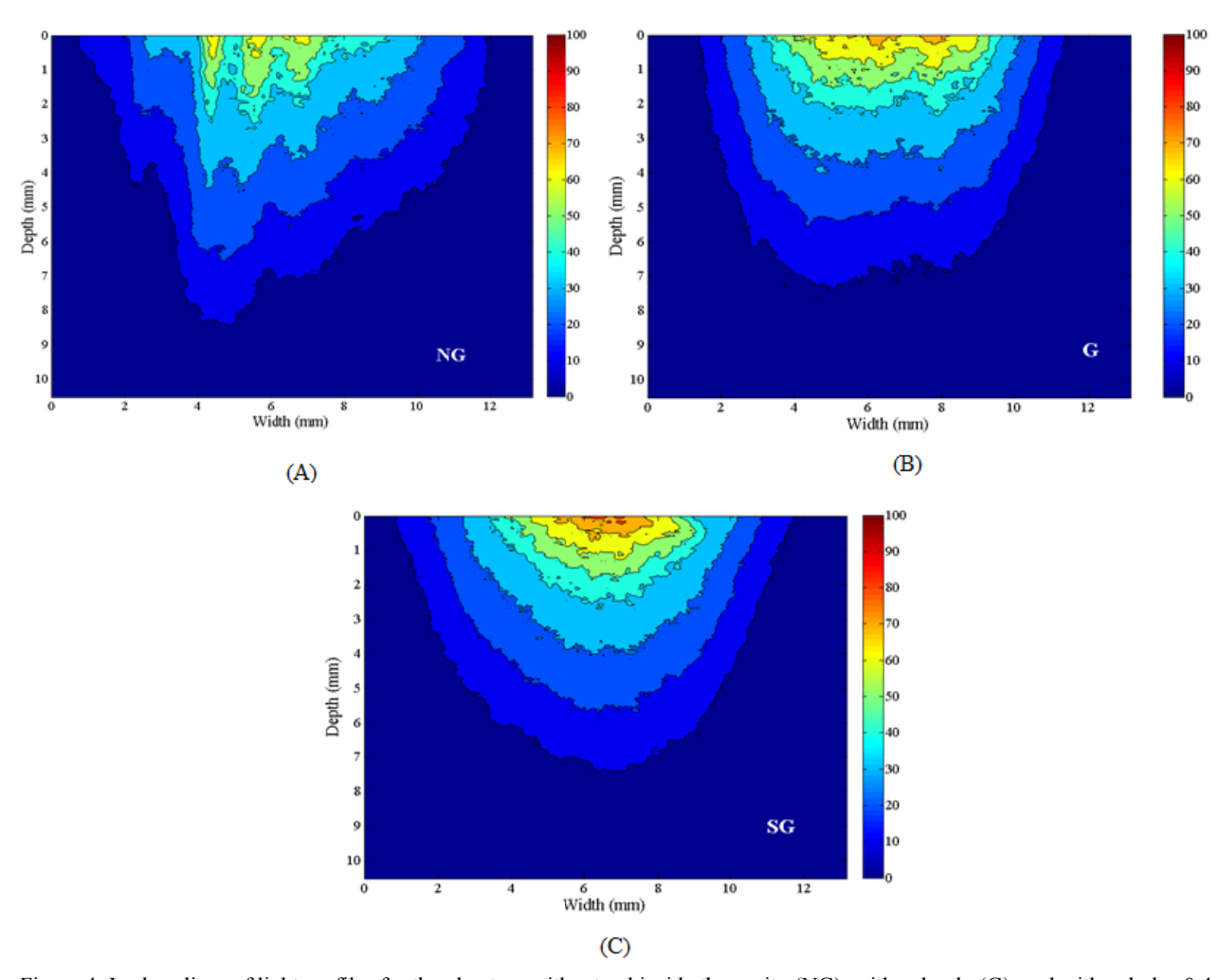


Figure 4: Isodose lines of light profiles for the phantom without gel inside the cavity (NG), with gel only (G), and with gel plus 0.4 μ l/g of the scattering agent Lipofundin®(SG).

To quantify the uniformity of these distributions, a line was traced perpendicularly to the direction of propagation of the beam, 2 mm below the surface of the phantom, which is the average penetration of light in tissue when using 630 nm ²⁶. Values of intensity were obtained according to the position, generating the curves shown in Figure 5, which were compared to a Gaussian fitting. The experimental curves were adjusted to a Gaussian. The R² parameter²⁷, which is a measurement of the statistical fitting of the model function to the experimental curve, was used as a comparison parameter, since the closer the R² coefficient is to 1, the better is the fitting. The situation with the best fitting to a Gaussian was the curve for SG (Figure 5c). This is an important evidence of the increase in homogeneity that the use of a slightly scattering gel may provide in tissue irradiation.

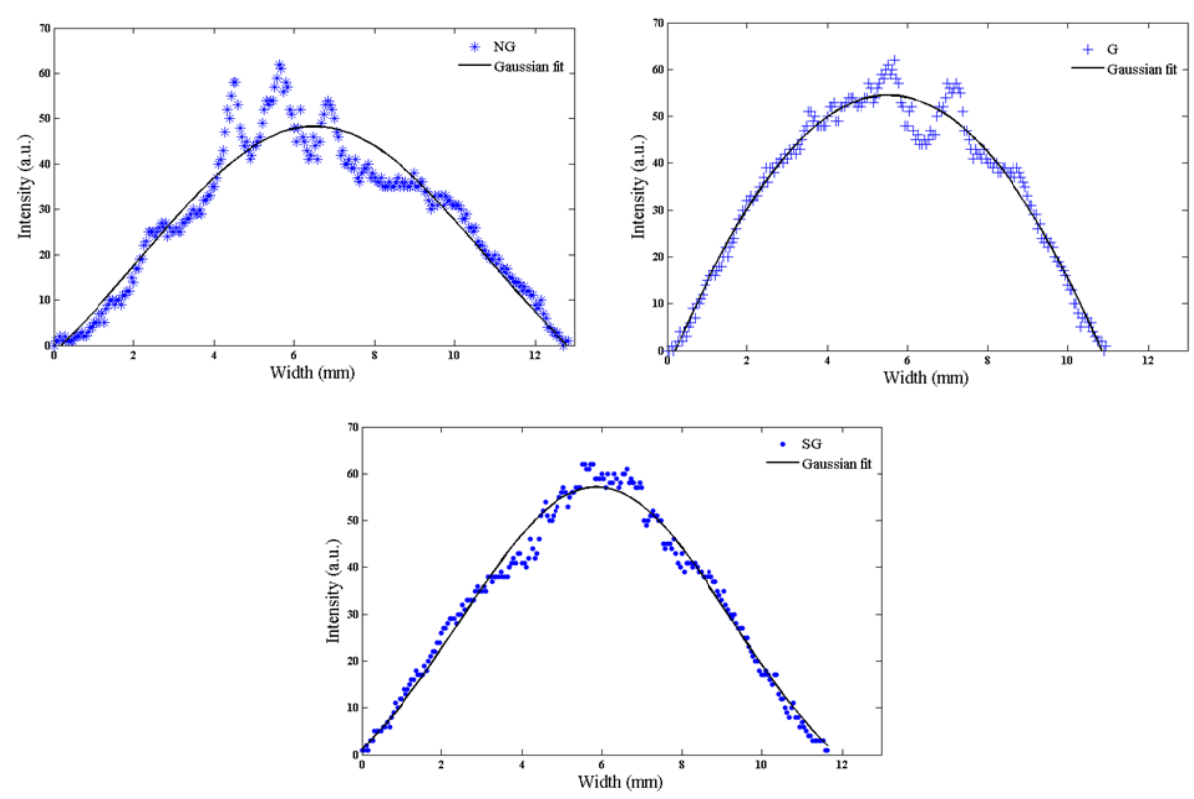


Figure 5: Comparison uniformity for no gel (NG, $R^2 = 0.91967$), gel-only (G, $R^2 = 0.97115$) and gel plus scattering agents (SG, $R^2 = 0.98078$) configurations, at 2.0 mm depth.

Aiming to further analysis, Figure 6 represents the adequacy of the curve fitting to the light profiles in different depths, concerning each of the three conditions of light coupling. This adequacy is represented by the parameter R², or the coefficient of multiple determination for multiple regression, which is a statistical parameter that measures how close the actual data are to a fitted regression line. Here, the light profile was extracted for several penetration depths, to examine regions with larger and smaller intensities. The R² values, related to the profiles for several depths of each of the NG, G, and SG setups, are shown (Figure 6). When there is no gel present in the hollow cavity, surface irregularities create large fluctuations, as one can see in the profiles of Figure 5 and Figure 2. The consequence is that these significant imperfections in intensity are not compensated by the scattering, so it is observed for considerable depths. When deeper penetration is reached (about 3 mm), though, attenuation and scattering events become more important, and such imperfections are more and more compensated. Thus, R² at this point increases again, since matching between fit and data increases.

For the case of gel without the scattering agent, the coupling is significantly improved, since reflection is attenuated. However, although reduced by the presence of gel, the light beam profile is still heterogeneous within the phantom. When, light diffusion in the gel is increased by the scattering agent, part of the photons is redirected from the propagation direction before they reach the target. Thus, the light incidence occurs on a variety of angles, increasing the number of photons that couple to the interface in an angle that favors transmission. This hence improves their ability to bypass surface irregularities that ultimately promote the severe fluctuations in intensity, propagating throughout the media. Therefore, the light is delivered more uniformly, and the fluctuation effects that occur in the medium are less evident for a much larger depth. With that, the uniformity of the light distribution in the phantom remains well preserved, without greatly compromising the intensity delivered.

This comparison shows that in the presence of the gel with scattering agents, the curve intensities become much more regular than in the other cases, especially with the increase of depth. Another important observation was that the R² values remain almost unchanged for the SG setting, which means that along the phantom depth, the Gaussian nature of the propagating beam does not change. In contrast, the effect of not using the gel was noticeable, with the lowest matching of the fitting curve to data. Even for the gel alone, for very short penetration the R² parameter approaches the gel with scatterer results, but there is an important decrease of R² starting from 1.5 mm in depth. It is also worth to mention that the R² value becomes more and more similar for SG and G groups, which represents the predominance of the effect of the medium scattering on light with depth, which makes the behavior of light going more and more similar. This effect is not observed for the penetration range investigated, but there is a slight tendency of R² to reduce with the increase of depth for the SG group, which reinforces the interpretation of the medium scattering effect to be responsible for the reduction of the fitting-data match. However, it clearly shows the importance of the contribution that this gel plus scatter may represent in light coupling for rough surfaces. Moreover, this feature is essential to the optimization of phototherapy techniques and, particularly, for PDT applications.

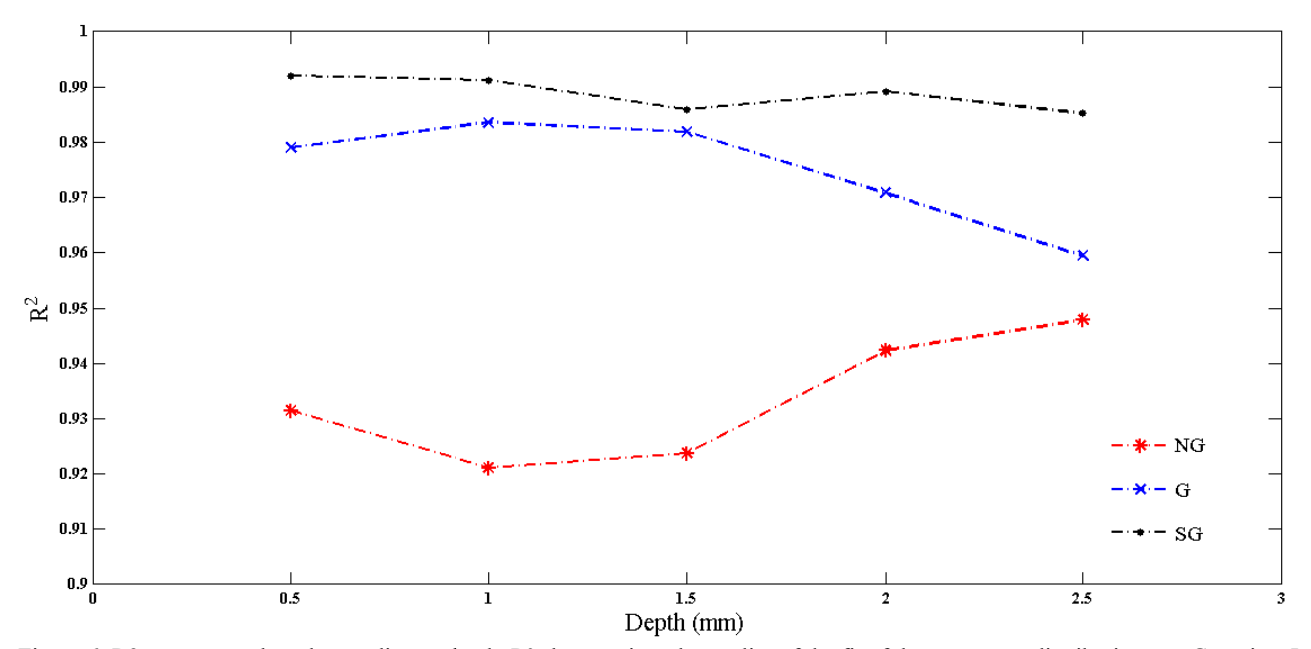


Figure 6: R2 parameter plotted according to depth. R2 characterizes the quality of the fit of the transverse distribution to a Gaussian. It shows that the behavior for the gel plus scatterer agent is so that the distribution inside the phantom better matches the profile of the beam, meaning that it is more Gaussian along the depth.

The parameter W is the estimated beam width, which is related to the focalization of the light inside the phantom. This width W corresponds to the waist of the Gaussian beam obtained by fitting (1). The evolution of the beam width is represented in Fig 7.

$$y = y_o + \sqrt{\frac{2}{\pi}} \frac{A}{w} exp \left[-2 \left(\frac{x - x_c}{w} \right)^2 \right]$$
 (1)

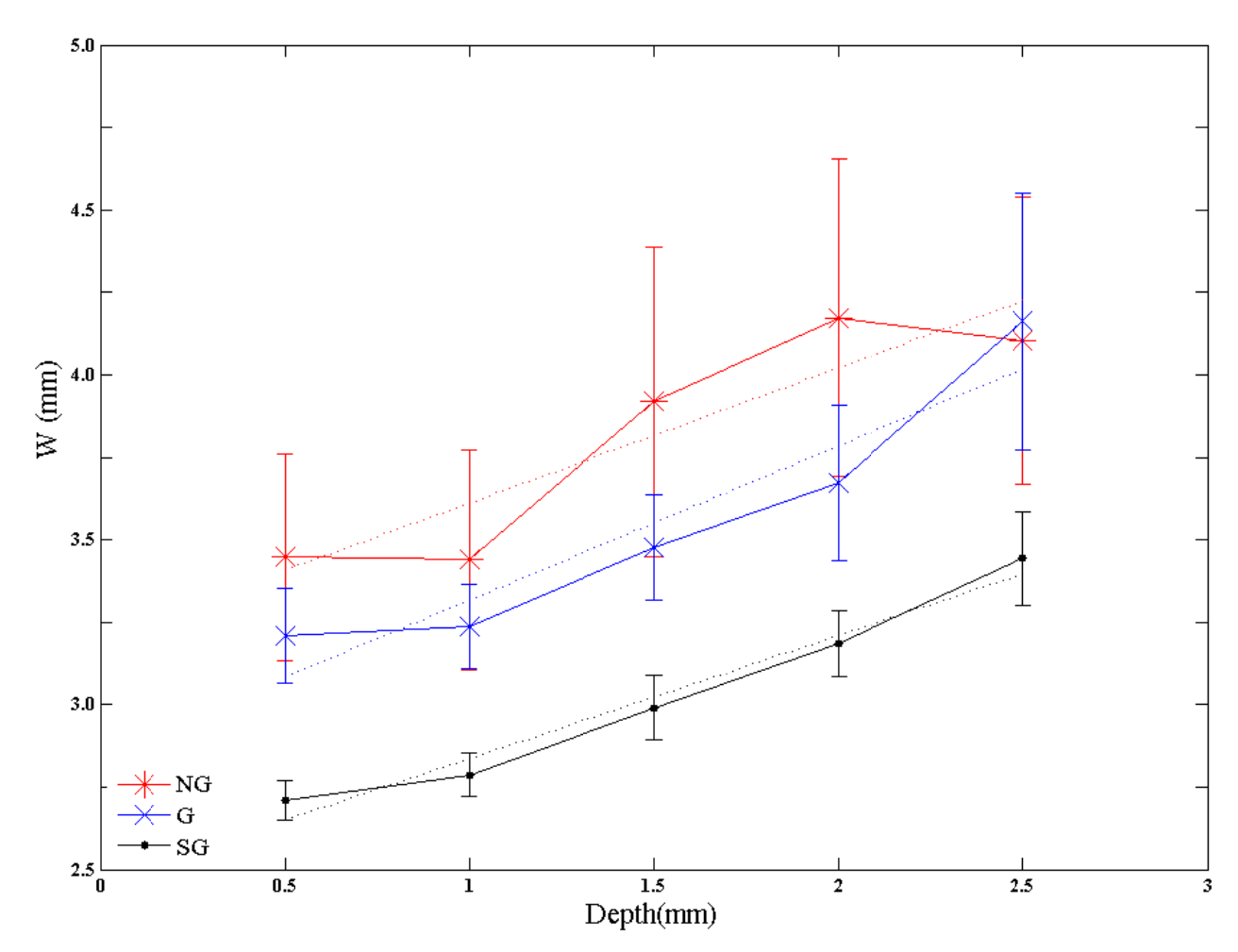


Figure 7: Scattering parameter given by W (Gaussian width) for different curves along the depth of the phantom.

One can observe from Figure 7 that in the SG configuration, the beam width is significantly smaller than in the other cases. The W parameter values for every assessed depth are more homogeneous for gel tests than for non-gel tests (which can be seen by the error bars). For those, W varies linearly, whereas for measurements without gel such linearity is not observed, as can be seen, based on the linear fitting.

On the other hand, the linear fitting slopes show minor difference, which is expected since the way the beam is distorted depends basically on the optical properties of the medium it is propagating in, and not of the light coupling agents by the interface; that is evidence that the gel methods do not modify the phantom itself, but only the light propagating through the interface.

Furthermore, the smaller W values observed for gel groups, especially SG, imply in larger light penetration into the phantom. Considering clinical applications, it would favor the treatment of deeper lesions, given the reduced light beam dispersion.

Therefore, the data presented in figure 7 shows that presence of the scatters in the coupling gel plays an important role in keeping the beam more regular during its propagation within the phantom.

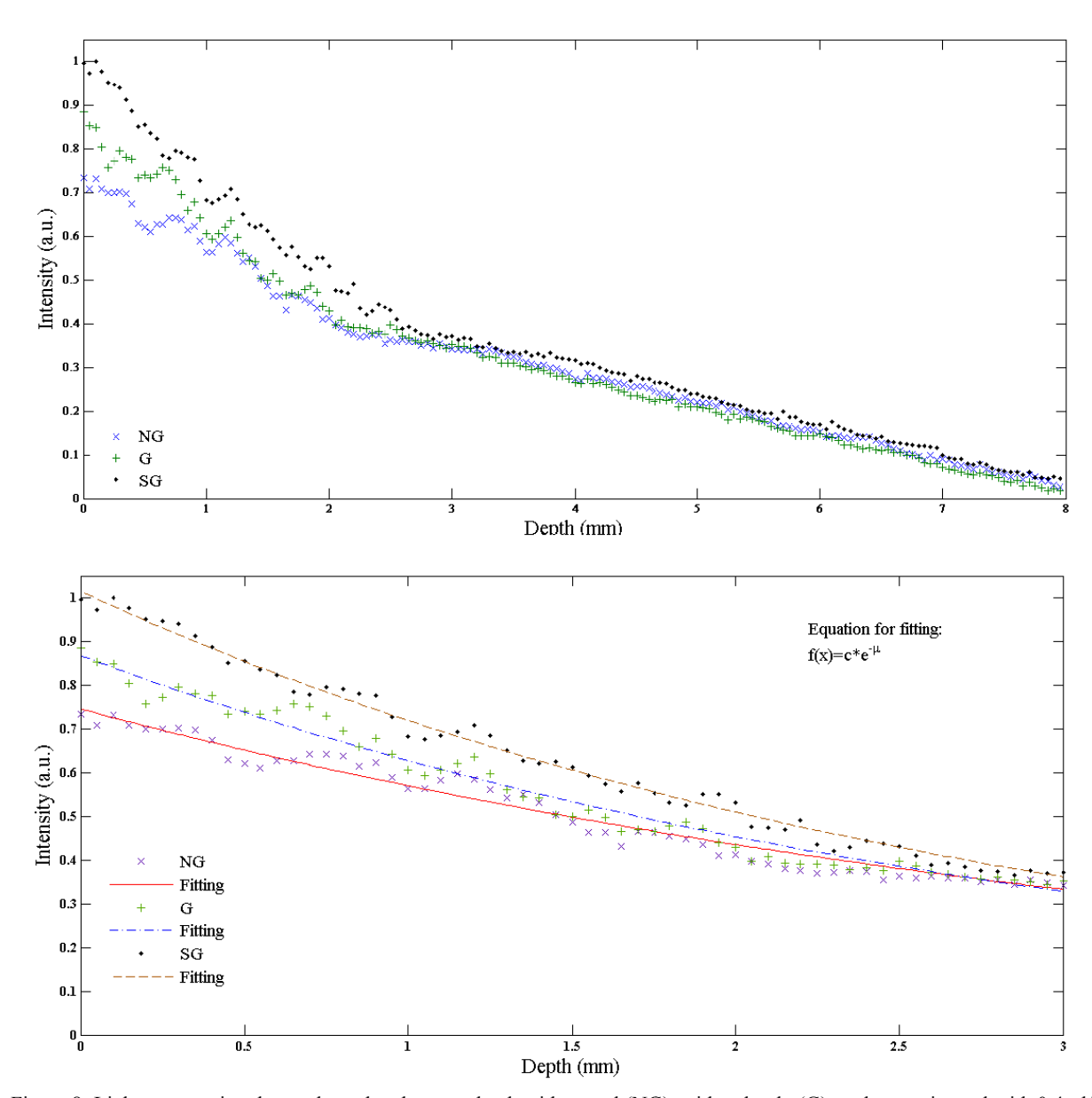


Figure 8: Light propagation decay along the phantom depth without gel (NG), with gel only (G), and scattering gel with 0.4 μ l/g of Lipofundin® (SG) (above); detail for the range 0-3 mm, including exponential fitting (below).

For cases where the cavity was filled with gel (either G or GS), the light intensity just below the interface is greater (Figure 8). However, even considering the losses occurring due to the passage of light through the coupler gel (i.e., by scattering), light reflection at the interface air/phantom (without gel) is the effect that leads to higher losses. Since reflections are caused by wave vector mismatch, and the wave vectors are determinate by the refractive indices, covering a surface with a layer of coupling material results in lower reflection rates and increased transmission of light through the surface interface²⁸. The decay constant (μ) for each of the exponential fittings is different. The value for NG constant ($\mu_{ng} = -0.27 \pm 0.01$) is smaller than for gel, and for the SG is higher ($\mu_{sg} = -0.350 \pm 0.008$) than for G

only ($\mu_g = -0.33 \pm 0.01$). That shows how the presence of a coupling agent positively interferes with the light propagation within the phantom.

To evaluate the uniformity of spatial distribution of light, isodose curves data for a distance of 2 mm from the irradiation spot were compared to the fitting by parables, and the light intensity values for the specific points on these parables were evaluated. This comparison aims to show how the heterogeneities may interfere with phototherapies in general, and how the use of the gel as a coupling tool may contribute to reducing this effect. Thus, when comparing the values of the actual intensity values and those obtained for the fitted parable, a smaller difference between them means more uniformity. The observation on the fluctuation around an average value of intensity was considered to assess the delivery of a specific amount of energy at a given depth. We have considered the curves for an energy dose of 40 J/cm², because this is the minimum amount of energy to be delivered to the skin for the elimination of carcinoma by PDT using a porphyrin as a photosensitizer and a 630 nm light source as treatment light²9. This light dose for PDT was chosen to represent that because this is one of the treatment situations in which not achieving the proper treatment may result in the severe complication of the clinical condition of the patient, by allowing a recurrence to happen. The referred doses are presented in Figure 9.

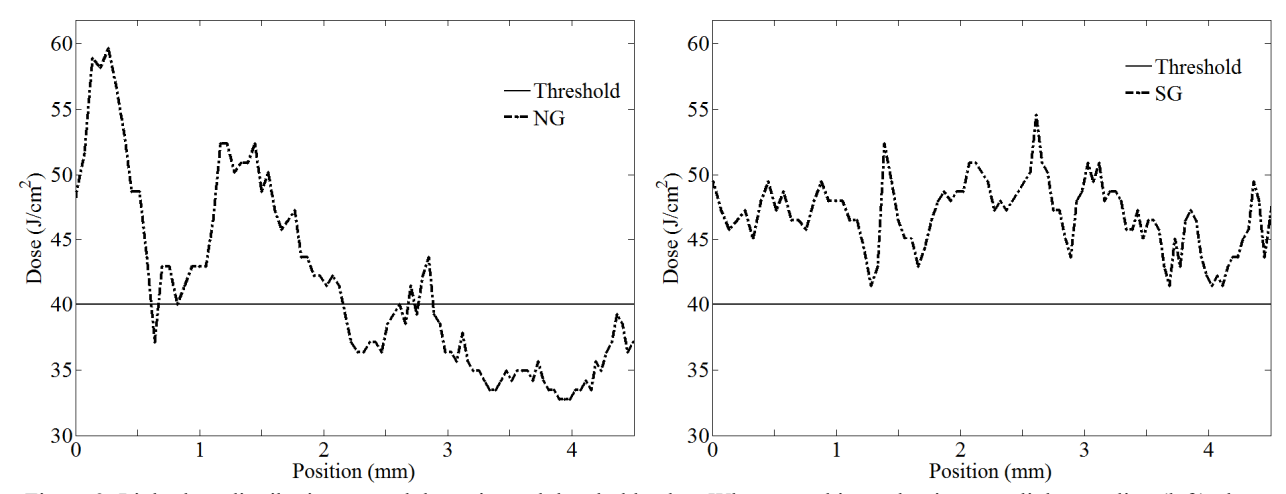


Figure 9: Light dose distribution around the estimated threshold value. When no gel is used to improve light coupling (left), the irregularities are much larger, and light delivery is much above or much below the threshold value, which does not happen for the SG condition (right).

The effects of phototherapies depend on the amount of fluence that is delivered to a tissue bulk to be effective. Delivering a minimum amount of light to start or inhibit physical-chemical processes or reaction pathways is a requirement of any treatment based on a photoreaction or an excited-state reaction. This is particularly important for PDT, which is why the examples here shown are mostly based on it. In its case, achieving necrosis demands a threshold dose, which is the minimum one necessary to produce enough reactive species that will ensure the cells death³⁰. Obviously, if this amount is not reached, cells may survive, which could provoke a recurrent lesion later. On the case of other phototherapies, not reaching the minimum amount of light will not promote enough stimulation of organelles and/or cell membrane structures to start desired or stop undesired metabolic events in the treated cells, also jeopardizing the treatment.

In Figure 9, both 9a and 9b, the solid line represents the threshold dose of 40 J/cm² that should supposedly be achieved at any point of the treated tissue, which is why this is represented by a horizontal line. The dashed line represents the measured dose obtained from data for both NG and SG situations. Of course, there is a natural fluctuation on the intensities that is detected at a specific distance from the irradiating source. This fluctuation range is very variable concerning neighbor points, and very dependent on the assessed position. However, the fluctuations observed for the NG situation range from 32-60 J/cm², whereas the SG situation shows fluctuation ranging from 41-55 J/cm².

Even more importantly, for SG situation, at any assessed point, all the values are above 40 J/cm², in contrast to those for NG, in which the presence of irregularities imply that only a few regions satisfy the criterion mentioned above while others are below that. The regions for which the dose is below threshold line are a real concern, because they mean that there are points where the tissue receives much larger-than-necessary light doses, which may eventually carry out undesired effects such as thermal ones, and despite it, there are points for which the minimum to promote proper treatment is not delivered, with deleterious consequences such as those discussed above, like leaving behind viable tumor cells. If tumor cells are present in those regions, the recurrence will occur. In fact, in previous experiments performed by our group³¹, islands of growing cells within the PDT treated region were observed. Then, those regions where associated with illumination irregularities induced by the presence of blood vessels in the tissue. As one can see in Figure 9(a), the regions below the threshold might be an example of the cause of those groups of surviving cells. That is quite important for approaches such as PDT skin cancer.

In the case of phototherapies in general, the most suitable way to ensure adequate treatment is by establishing proper dosimetry. Managing dosimetry for tissue irradiation is much more straightforward and, hence, feasible, in cases that light delivery is possible to predict and control, which is easier when light distribution in tissue is more isotropic. Therefore, the results here shown represent a significant stimulus to the use of this approach to improve light delivery for phototherapies.

IV. CONCLUSIONS

We have presented in this study a possible application to improve PDT outcome for surface tumors and to ensure proper protocol implementation for phototherapies. The use of Carbopol gel with addition of lipidic emulsion provides an effective improvement in the illumination uniformity, removing effects caused by the roughness of the tissue surface. Light propagation was less disturbed by the surface roughness since there was a decrease in the difference between the refractive indexes of the phantom and the medium light was coming from. Since the refractive index of the phantom was around 1.333 and for the coupling gel is 1.338, the interface transmission was more efficient. The increased scattering in the light source medium also contributed to the increased homogeneity by allowing photons to be delivered from several angles, thus contributing to better light/phantom coupling.

The depth reached by light was also larger when SG was used, when compared to the gel alone, which may be explained by the return of reflected photons to the interface due to scattering within the gel at SG.

As a final remark, using a gel to improve irradiation effectiveness is quite easy considering most protocols, which makes this approach a real option for the improvement of clinical treatment using optical techniques. Further studies shall produce *in vivo* evidence of such improvements and will be presented soon.

V. ACKNOWLEDGEMENT

The authors acknowledge the support provided by Brazilian Funding Agencies: Capes; CNPq and São Paulo Research Foundation (FAPESP) grants: 2013/07276-1 (CEPOF), 2014/50857-8 (INCT).

REFERENCES:

- [1] Prof, A. E., "Light transport in tissue," Appl. Opt. **28**(12), 2216–2222 (1989).
- Yessayan, D., Zacharakis, G. and Ntziachristos, V., "Experimental determination of photon propagation in highly absorbing and scattering media," 546–551 (2005).
- [3] Moriyama, L. T., Lins, E. C. C., Kurachi, C. and Bagnato, V. S., "Light distribution in turbid media: an approach based on matrices," Proc. SPIE **7886**, D. H. Kessel and T. Hasan, Eds., 788615–788615–4 (2011).
- [4] Flock, S. T., Wilson, B. C. and Patterson, M. S., "Monte Carlo modeling of light propagation in highly scattering tissues--II: Comparison with measurements in phantoms.," IEEE Trans. Biomed. Eng. **36**(12), 1169–1173 (1989).
- [5] Flock, S. T., Patterson, M. S., Wilson, B. C. and Wyman, D. R., "Monte Carlo modeling of light propagation in highly scattering tissue--I: Model predictions and comparison with diffusion theory.," IEEE Trans. Biomed. Eng. **36**(12), 1162–1168 (1989).
- [6] Gardner, C. M., Jacques, S. L. and Welch, a J., "Light transport in tissue: Accurate expressions for one-dimensional fluence rate and escape function based upon monte carlo simulation.," Lasers Surg. Med. **18**(2), 129–138 (1996).
- [7] Grecco, C., Buzzá, H. H., Stringasci, M. D., Andrade, C. T., Vollet-Filho, J. D., Pratavieira, S., Zanchin, A. L., Tuboy, A. M. and Bagnato, V. S., "Single LED-based device to perform widefield fluorescence imaging and photodynamic therapy," SPIE Biophotonics South Am. Int. Soc. Opt. Photonics **9531**, 953121 (2015).
- [8] Jerjes, W. K., Upile, T., Wong, B. J., Betz, C. S., Sterenborg, H. J., Witjes, M. J., Berg, K., Veen, R. Van, Biel, M. A., El-naggar, A. K., Mosse, C. A., Olivo, M., Richards-kortum, R., Robinson, D. J., Rosen, J., Yodh, A. G., Bigio, I., Chen, Z., Cruz, A. K. D., et al., "The future of medical diagnostics: review paper," 1–9 (2011).
- [9] Choudhary, S., Nouri, K. and Elsaie, M. L., "Photodynamic therapy in dermatology: A review," Lasers Med. Sci. **24**(6), 971–980 (2009).
- [10] Brown, S. B., Brown, E. A. and Walker, I., "Review The present and future role of photodynamic therapy in cancer treatment Photodynamic therapy" (2004).
- [11] Lindberg-Larsen, R., Sølvsten, H. and Kragbale, K., "Evaluation of recurrence after photodynamic therapy with topical methylaminolaevulinate for 157 basal cell carcinomas in 90 patients," Acta Derm. Venereol. **92**(2), 144–147 (2012).
- [12] Asakage, T., Yokose, T., Mukai, K., Tsugane, S., Tsubono, Y., Asai, M. and Ebihara, S., "Tumor thickness predicts cervical metastasis in patients with Stage I/II carcinoma of the tongue," Cancer **82**(8), 1443–1448 (1998).
- [13] Allison, R. R., Sibata, C. H., Downie, G. H. and Cuenca, R. E., "A clinical review of PDT for cutaneous malignancies," Photodiagnosis Photodyn. Ther. **3**(4), 214–226 (2006).
- [14] SIMUNOVIC, Z., "Low Level Laser Therapy with Trigger Points Technique: A Clinical Study on 243 Patients," J. Clin. Laser Med. Surg. 14(4), 163–167 (1996).
- [15] Liu, B.-S., Huang, T.-B. and Chan, S.-C., "Roles of reinforced nerve conduits and low-level laser phototherapy for long gap peripheral nerve repair," Neural Regen. Res. 9(12), 1180–1182 (2014).
- [16] Marcuse, D., [Light transmission optics], Van Nostrand Reinhold, New York (1972).
- [17] Weir, V. M. and Woo, T. Y., "Photo-assisted epilation—review and personal observations," J. Cutan. Laser Ther. **1**(3), 135–143 (1999).
- [18] Gold, M. H., Bell, M. W., Foster, T. D. and Street, S., "Long-term epilation using the EpiLight broad band, intense pulsed light hair removal system," Dermatol Surg **23**(10), 909–913 (1997).
- [19] Prokop, A. F., Vaezy, S., Noble, M. L., Kaczkowski, P. J., Martin, R. W. and Crum, L. A., "Polyacrylamide gel as an acoustic coupling medium for focused ultrasound therapy," Ultrasound Med. Biol. **29**(9), 1351–1358

- (2003).
- [20] Galanzha, E. I., Tuchin, V. V, Solovieva, A. V, Stepanova, T. V, Luo, Q. and Cheng, H., "Skin backreflectance and microvascular system functioning at the action of osmotic agents," J. Phys. D. Appl. Phys. **36**(14), 1739 (2003).
- [21] Michels, R., Foschum, F. and Kienle, A., "Optical properties of fat emulsions Abstract:," 2304–2314 (2008).
- [22] Cubeddu, R., Pifferi, A., Taroni, P. and Torricelli, A., "A solid tissue phantom for photon migration studies," Phys. Med. Biol. **42**, 1971–1979 (1997).
- [23] Madsen, S. J., Patterson, M. S. and Wilson, B. C., "The use of India ink as an optical absorber in tissue-simulating phantoms," Phys. Med. Biol. **37**(4), 985 (1992).
- [24] Hosmani, A. H., Thorat, Y. S. and Kasture, P. V., "Carbopol and its pharmaceutical significance: a review," Pharmainfo. net 4(5) (2006).
- [25] McKenzie, a L. and Byrne, P. O., "Can photography be used to measure isodose distributions of space irradiance for laser photodynamic therapy?," Phys. Med. Biol. **33**(1), 113–131 (1988).
- [26] Valentine, R. M., Wood, K., Brown, C. T. a, Ibbotson, S. H. and Moseley, H., "Monte Carlo simulations for optimal light delivery in photodynamic therapy of non-melanoma skin cancer.," Phys. Med. Biol. **57**(20), 6327–6345 (2012).
- [27] Eisenhauer, J. G., "Regression through the origin," Teach. Stat. 25(3), 76–80 (2003).
- [28] Lekner, J. and Dorf, M. C., "Why some things are darker when wet," Appl. Opt. 27(7), 1278–1280 (1988).
- [29] Sabino, L. G., de Negreiros, L. M. V., Vollet-Filho, J. D., Ferreira, J., Tirapelli, D. P. C., Novais, P. C., Tirapelli, L. F., Kurachi, C. and Bagnato, V. S., "Experimental evidence and model explanation for cell population characteristics modification when applying sequential photodynamic therapy," Laser Phys. Lett. 8(3), 239–246 (2011).
- [30] Ramirez, D. P., Kurachi, C., Inada, N. M., Moriyama, L. T., Salvio, A. G., Vollet Filho, J. D., Pires, L., Buzzá, H. H., de Andrade, C. T., Greco, C. and Bagnato, V. S., "Experience and BCC subtypes as determinants of MAL-PDT response: preliminary results of a national Brazilian project.," Photodiagnosis Photodyn. Ther. **11**(1), 22–26 (2014).
- [31] Ferreira, J., Kurachi, C., Zucoloto, S., e Silva, O. C. and Bagnato, V. S., "Islands of surviving cells within necrotic volume at liver induced by PDT," Photodyn. Ther. Back to Futur. **7380**, 73803S, International Society for Optics and Photonics (2009).